The Journal of Chemical Physics

Temperature dependence of water-water and ion-water correlations in bulk water and electrolyte solutions probed by femtosecond elastic second harmonic scattering

Cite as: J. Chem. Phys. **148**, 222835 (2018); https://doi.org/10.1063/1.5023343
Submitted: 23 January 2018 . Accepted: 09 April 2018 . Published Online: 30 April 2018

Yixing Chen, Nathan Dupertuis, Halil I. Okur, and Sylvie Roke

Temperature dependence of water-water and ion-water correlations in bulk water and electrolyte solutions probed by femtosecond elastic second harmonic scattering

Yixing Chen,[a] Nathan Dupertuis,[a] Halil I. Okur, and Sylvie Roke[b]
Laboratory for Fundamental BioPhotonics (LBP), Institute of Bioengineering (IBI), Institute of Materials Science (IMX), School of Engineering (STI), and Lausanne Centre for Ultrafast Science (LACUS), École Polytechnique Fédérale de Lausanne (EPFL), CH-1015, Lausanne, Switzerland

(Received 23 January 2018; accepted 9 April 2018; published online 30 April 2018)

The temperature dependence of the femtosecond elastic second harmonic scattering (fs-ESHS) response of bulk light and heavy water and their electrolyte solutions is presented. We observe clear temperature dependent changes in the hydrogen (H)-bond network of water that show a decrease in the orientational order of water with increasing temperature. Although D_2O has a more structured H-bond network (giving rise to more fs-ESHS intensity), the relative temperature dependence is larger in H_2O. The changes are interpreted in terms of the symmetry of H-bonds and are indicators of nuclear quantum effects. Increasing the temperature in electrolyte solutions decreases the influence of the total electrostatic field from ions on the water-water correlations, as expected from Debye-Hückel theory, since the Debye length becomes longer. The effects are, however, 1.9 times (6.3 times) larger than those predicted for H_2O (D_2O). Since fs-ESHS responses can be computed from known molecular coordinates, our observations provide a unique opportunity to refine quantum mechanical models of water.
https://doi.org/10.1063/1.5023343

INTRODUCTION

Water in its liquid form is the medium of life. In organisms, the structural building blocks of cells (lipid membranes, proteins, DNA, etc.) are embedded in electrolyte solutions. The structure of water and the hydration of ions have continuously been of high interest as they are involved in numerous physiological, medical, biological, and chemical processes.[1] Examples are protein folding/precipitation, enzyme, ion channel, and ion pump activity, action and membrane potential generation, transport across membranes, self-assembly, interfacial charging, and aerosol formation.[1–6] Most studies of ion-water interactions have focused on concentrations above 0.1 M, and from these studies it has emerged that ion specific water-ion interactions occur over up to 3 hydration shells.[7–17] Recently, femtosecond elastic second harmonic scattering (fs-ESHS) experiments, in combination with reflection second harmonic generation and surface tension measurements,[18] have shown that there is also an interaction that ranges over tens of hydrations shells and displays significant nuclear quantum effects.[19–26] This effect involves the interaction of the combined electrostatic field of all the ions with the hydrogen (H)-bond network in solution.[18,21,27] The orientational correlations or orientational order between the water molecules increases in response to an ionic electrostatic field, leading to an increase in the fs-ESHS response (as in Fig. 1), a decrease in the surface tension, and an increase in the dielectric energy of the bulk medium.[28] Although the qualitative ingredients of this behavior are understood, there are still many open questions. In the present work, we provide a further experimental investigation into the temperature dependence of the fs-ESHS response of bulk light and heavy water and their electrolyte solutions.

With fs-ESHS, we probe the second harmonic (SH) response of liquid molecules. The measured SH intensity originates from electronic anisotropy within every single non-spherical molecule and is modified by orientational correlations of the non-spherical molecules. Randomly distributed liquid molecules as in an ideal gas are uncorrelated with each other; second harmonic scattering (SHS) from these uncorrelated molecules is an incoherent sum of the SH response of individual molecules, which is also referred to as hyper-Rayleigh scattering (HRS). Molecular correlations can be induced by H-bonding, Coulombic interaction, dipole-dipole interaction, or other interactions. For water, the orientational correlation of a pair of water molecules can be changed by breaking an H-bond through a rotational or bending/libration motion, but not by stretching (see the inset in Fig. 1). The orientational correlation modifies the coherent contribution of the correlated molecules to the SH intensity. Note that femtosecond laser pulses that are shorter than the orientational relaxation time of water are necessary to measure snapshots of the static collective orientational correlations in water. As shown in Ref. 18, information on the two origins of SH responses can be obtained from the SH intensity measured in different polarization combinations of the

[a]Y. Chen and N. Dupertuis contributed equally to this work.
[b]sylvie.roke@epfl.ch

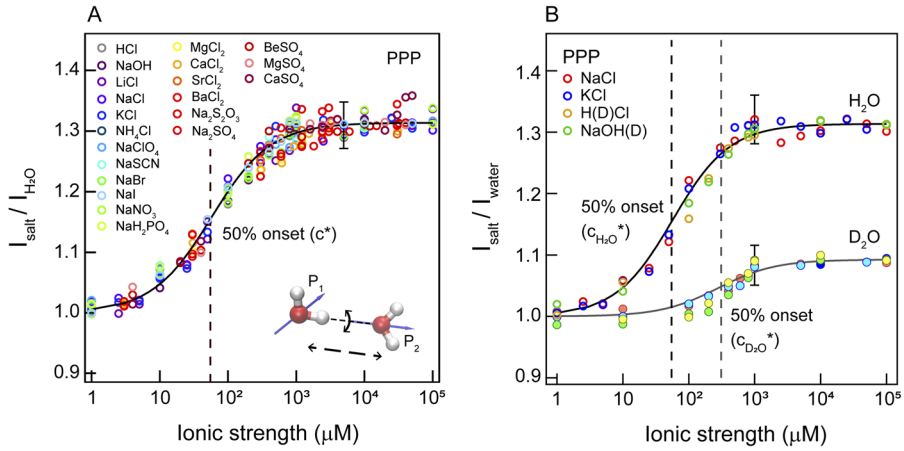

FIG. 1. Fs-ESHS of electrolyte solutions at room temperature. (a) fs-ESHS intensities, relative to that of pure water, of 21 different electrolyte solutions obtained at a scattering angle of 90° (PPP polarization combination). The relative intensities of all electrolyte solutions can be fit with a Langmuir equation whose functional form is given by $\Delta I = A\frac{(c/c^*)}{1+(c/c^*)}$, with c as the ion concentration and A as a fitting parameter. The dashed line indicates the concentration of half saturation, c^*, which is extracted from the fitting. The fs-ESHS data are adapted from Ref. 18. The inset illustrates two H-bonded water molecules that are orientationally correlated. The black arrows represent different axes along which H-bonds can be broken. fs-ESHS is mostly sensitive to the breaking of this H-bond via rotation (black curved arrow). In the D_2O molecule, the H-bond bending mode is predicted to be stronger than in H_2O, due to nuclear quantum effects. Oppositely, the H-bond stretching mode is expected to be weaker. (b) fs-ESHS intensities of NaCl, KCl, H(D)Cl, and NaOH(D) in H_2O and D_2O (PPP polarization combination). The H_2O (D_2O) data are normalized to pure H_2O (D_2O).

incident and scattered light. The polarization combinations are indicated with a three letter code, from left to right, representing the polarization of the scattered SH light and the incident fundamental light with P(S) referring to linearly polarized light parallel (perpendicular) to the scattering plane. The PPP and PSS combinations mainly report on the collective orientational order, and the SH intensity consists of both coherent contributions from correlated molecules and incoherent contributions from uncorrelated molecules. The SSS and SPP combinations report on the electronic structure of individual molecules, and the SH intensity is dominated by the incoherent contributions from uncorrelated molecules. According to the selection rule of SHS, molecular correlations of spherical symmetry only contribute to the PPP and PSS SH intensities.[29]

Figure 1(a) shows the relative change of the PPP fs-ESHS intensity (at scattering angle $\theta = 90°$) for 21 different electrolyte solutions in the ionic strength range of 1 μM–0.1M, as reproduced from Ref. 18. The SH intensity was recorded at room temperature (296.15 K, 23 °C). The 21 electrolytes include a monovalent Cl^- cation series (NH_4Cl, KCl, NaCl, LiCl, and HCl), an Na^+ anion series (NaH_2PO_4, NaOH, NaCl, NaBr, NaI, $NaNO_3$, $NaClO_4$, and NaSCN), divalent cationic–monovalent anionic pairs ($MgCl_2$, $CaCl_2$, $SrCl_2$, and $BaCl_2$), monovalent cationic-divalent anionic pairs ($Na_2S_2O_3$ and Na_2SO_4), and divalent cationic-anionic pairs ($BeSO_4$, $MgSO_4$, and $CaSO_4$). For all electrolyte solutions, the same trend in the SH intensity is observed: A continuous rise up to a plateau with a saturated increase by 30% ± 3%. The 50% half-saturation concentration (c^*) is at 55 ± 5 μM. This non-ion-specific, saturated increase in the PPP fs-ESHS intensity indicates that electrolytes induce orientational order in the H-bond network of bulk water that extends over tens of hydration shells. Figure 1(b) shows a comparison of the PPP fs-ESHS intensity of NaCl dissolved in H_2O and NaCl, KCl, DCl, and NaOD dissolved in D_2O. A similar trend in the SH intensity is observed for the D_2O solution, but the intensity changes up to the plateau are only 9% ± 3% with $c^* = 310 \pm 71$ μM. Additional electrolyte solutions in D_2O display the same behavior as NaCl solutions [Fig. 1(b)]. Provided that the differences in the linear dielectric properties of H_2O and D_2O are minimal, such as permanent dipole moment and dielectric constant, this significant difference in the SH response is a manifestation of stronger H-bonding in D_2O than in H_2O, which arises from nuclear quantum effects.[19–22,25,26,30–36] It also indicates the importance of collective H-bonding.[18] Since these studies clearly show the importance of H-bonding and since temperature can modify the probability that H-bonds are formed and broken,[37] it is of interest to investigate the above behavior for different temperatures.

Here we investigate the temperature dependence of the fs-ESHS response of bulk H_2O and D_2O as well as NaCl solutions in light and heavy water. We find that bulk light and heavy water both display a reduction in their intermolecular coherent responses as the temperature is increased from 263.35 K (−9.8 °C) to 321.45 K (48.3 °C). However, both liquids have distinct temperature behaviors with a larger intermolecular coherent contribution in D_2O arising from stronger spherically symmetric orientational correlations in the H-bond network. The relative temperature dependent change is bigger for H_2O than for D_2O. For electrolyte solutions, the intensity vs temperature curves, such as recorded in Fig. 1(b), shift to higher ionic strengths due to a decreased screening of the electrostatic field at higher temperatures as explained by the Debye-Hückel theory. However, the half-saturation concentrations change more than the model prediction, with D_2O deviating by a factor of 6.3 and H_2O by a factor of 1.9. These measurements display the complexity of liquid water and provide a challenge for future models of water and electrolyte solutions.

MATERIALS AND METHODS

Sample preparations

NaCl (99.999%, Sigma-Aldrich), KCl (99.999%, Acros), NaOH (99.99%, Sigma-Aldrich), HCl (Ultrapure, Merck), NaOD solution (40 wt. % in D_2O, 99.5 at. % D, Sigma-Aldrich), and DCl solution (35 wt. % in D_2O, ≥99 at. % D, Sigma-Aldrich) were used as received without further purification. All samples were made by dissolving the electrolytes in degassed ultra-pure water to obtain a stock solution with a high concentration. For purifying H_2O, we used a Milli-Q UF plus instrument (Millipore, Inc.), with an electrical resistance of 18.2 MΩ cm. For the experiments with heavy water, we used degassed D_2O from Armar (99.8% d, > 2 MΩ cm). The stock solutions were filtered (0.1 μm polyvinylidene fluoride membrane filters, Millex-VV, Millipore) and diluted to the desired concentration.

Femtosecond elastic second harmonic scattering

Laser pulses (190 fs) centered at 1028 nm with a 200 kHz repetition rate were used as the light source for femtosecond elastic second harmonic scattering measurements. The polarization of the input pulses was controlled by a Glan-Taylor polarizer (GT10-B, Thorlabs) and a zero-order half wave plate (WPH05M-1030). The incident laser pulses, filtered by a long pass filter (FEL0750, Thorlabs), with a pulse energy of 0.3 μJ (incident laser power P = 60 mW) were focused into a cylindrical glass sample cell (4.2 mm inner diameter, LS instruments) with a waist diameter of ~35 μm and a Rayleigh length of 0.94 mm. The sample cell was placed in a customized temperature controller (Quantum Northwest) that provided a precise control of the temperature of the sample. The temperature can be tuned in the range of −253.15 K (−20 °C)–423.15 K (150 °C) with a precision of ±0.1 K. The scattered SH light was collected with a plano-convex lens (f = 5 cm) and then filtered by a bandpass filter (ET525/50, Chroma). A Glan-Taylor polarizer (GT10-A, Thorlabs) was used for the polarization analysis of the SH light. In the end, the SH light was focused into a gated photomultiplier tube (PMT) (H7421-40, Hamamatsu). The detection angle was set to 90° with an acceptance angle of 11.4°. For every data point, 3 to 11 measurements were performed and the averaged results are shown. In every measurement, the SH intensity was acquired with 50 × 1 s acquisition time (i.e., using $50 \times 2{\cdot}10^5$ pulses in total) and a gate width of 10 ns. The SH intensity of pure H_2O or D_2O (Figs. 1 and 3) was measured between every two samples and was used as a reference. The reproducibility of the fs-ESHS measurements is 1%–3%. Samples were stored and measured in sealed glass sample cells. The obtained relative intensities as a function of ionic strength were fit with a Langmuir-type equation derived from Debye-Hückel theory, whose functional form is given by $\Delta I = A\frac{(q\ell c^*)}{1+(q\ell c^*)}$, with c as the ion concentration and A as a fitting parameter. The 50% onset concentration c^* was extracted from the fitting. More details of fs-ESHS can be found in Ref. 38

RESULTS AND DISCUSSIONS

Temperature dependence of molecular correlations in water

Figure 2(a) shows the fs-ESHS intensities of pure H_2O and D_2O as a function of the temperature, measured in the PPP polarization combination. The plotted value is the intensity normalized by that at the highest temperature [T = 321.45 K (48.3 °C)]. Increasing the temperature from 263.35 K (−9.8 °C) to 321.45 K (48.3 °C), the PPP SH intensity drops by ~15% for H_2O and by ~10% for D_2O. The inset shows the measured intensities on the same scale. This shows that increasing the temperature of D_2O does not generate the same response as H_2O. In order to understand the behavior of Fig. 1(a) and to possibly assign it to changes in the orientational correlations in the H-bond network, we need to consider the sources of intensity change.

The SH intensity has two contributions: an intermolecular coherent and a molecular incoherent one. The temperature dependence of the incoherent response arises from the temperature dependence of the molecular hyperpolarizability and the dielectric constant that is connected to the local field factors. Thus, with increasing temperature, we may expect that the dielectric constant, the second-order hyperpolarizability, or the square of the second-order hyperpolarizability decreases or that the orientational correlations in the liquid become less probable. The dielectric constants of H_2O and D_2O differ by 0.5% at different temperatures,[39] and the hyperpolarizability is a reflection of the electronic structure of individual molecules and has been reported to be almost the same.[40] Therefore,

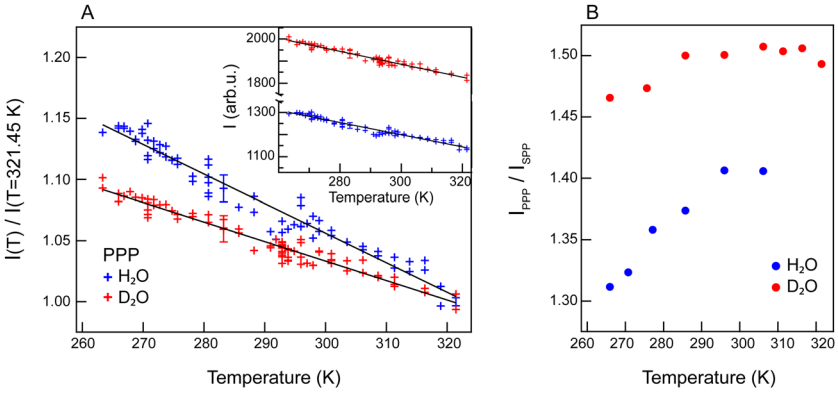

FIG. 2. Temperature dependent fs-ESHS of bulk light and heavy water. (a) fs-ESHS intensities of H_2O and D_2O as a function of temperature measured at a scattering angle of 90° (PPP polarization combination). The SH intensity is normalized by the intensity at 321.45 K (48.3 °C). The solid lines are guides to the eye. The inset displays the intensities of both liquids on the same intensity scale. (b) The ratio of the PPP intensity to the SPP intensity.

the difference in Fig. 1(a) stems from different degrees of intermolecular correlations between H_2O and D_2O. D_2O has more intermolecular correlations (or correlations that live longer), but changes less with temperature. This is consistent with the notion that D_2O has stronger H-bonds than H_2O.

In order to separate the molecular incoherent and intermolecular coherent contributions, we compare the response for PPP polarized light (that contains coherent and incoherent contributions for spherically symmetric systems) to the response for SPP polarized light (which contains only incoherent contributions). The incoherent contribution to the SH PPP and SPP intensity can be computed considering random uncorrelated point dipoles (with $\boldsymbol{p}_i^{(2)} = \boldsymbol{\beta}^{(2)} : \boldsymbol{E}(\omega)\boldsymbol{E}(\omega)$ the molecular second-order dipole moment for molecule i)[41,42]

$$I_{PPP}(2\omega) = \frac{cnk_0^4 N_m V E_x^4}{32\pi^2\epsilon_0 R^2}\left\{\left\langle\left(\beta_{yyy}^{(2)}\right)^2\right\rangle\cos^2\theta + \left\langle\left(\beta_{yxx}^{(2)}\right)^2\right\rangle\sin^2\theta\right\}, \quad (1)$$

$$I_{SPP}(2\omega) = \frac{cnk_0^4 N_m V E_x^4}{32\pi^2\epsilon_0 R^2}\left\langle\left(\beta_{yxx}^{(2)}\right)^2\right\rangle,$$

where c is the velocity of light in vacuum, n is the refractive index of air, k_0 represents the magnitude of the wavevector of the emitted SH light from the induced molecular dipole, E_x is the component of the electric field along the horizontal x-axis of the lab frame, orthogonal to the forward direction of incident laser beam (z-axis), θ is the scattering angle between the observation direction and the forward direction, N_m is the number density of the molecule, V is the volume in which molecules contribute to the SHS intensity and typically corresponds to the focal volume of the incident laser beam, R is the distance between the scattering point and the observation point, and $\beta_{ijk}^{(2)}$ corresponds to the values of molecular second-order hyperpolarizability tensor for different polarization combinations (ijk). Similar expressions can be found for the other polarization combinations.[42] For a molecular distribution with spherical symmetry, the SPP polarization combination contains only molecular contributions. The PPP polarized light generally contains both molecular and intermolecular contributions. Since at the used scattering angle ($\theta = 90°$) Eq. (1) is identical for both polarization combinations, dividing these at $\theta = 90°$ will thus remove the molecular incoherent contribution. The caveat here is that this works only for nonlinear optical scattering theory using spherical symmetry. This spherical symmetry refers to the spatial orientational distribution of H-bonded water molecules. A water molecule with 2 accepting and 2 donating H-bonds is spherically symmetric. A water molecule with a single accepting H bond is not spherically symmetric just like other H-bond-missing configurations. To go beyond this approximation requires extensive path integral molecular dynamics.[40]

Figure 2(b) shows the ratio of the measured PPP and SPP SH intensity at different temperatures. The temperature dependence of this intensity ratio is remarkably different compared to the PPP intensity shown in Fig. 2(a). Instead of continuously decreasing with increasing temperature, the intensity ratio of both liquids shows an increase and reaches saturation values at ~283.15 K (15 °C) for D_2O and ~293.15 K (20 °C) for H_2O, while H_2O shows a larger increase over the studied temperature range than D_2O. The intensity ratio of D_2O is larger than that of H_2O at all temperatures.

This different temperature dependence of the intensity ratio indicates a more complicated picture of the bulk water structure evolving with temperature than a mere change in the H-bond number. Breaking down the SH intensities, the SPP intensity consists primarily of an incoherent contribution from uncorrelated water molecules. We note that it could also contain a coherent contribution from orientationally correlated molecules that are distributed non-spherically as remarked above (as this is an approximation in the nonlinear optical theory[29]). By contrast, the PPP intensity contains a coherent contribution from spherically correlated molecules (and of non-spherically correlated molecules if the spatial distribution is non-spherical). We thus have two possible ratios ($R = I_{PPP}/I_{SPP}$) under the measurement condition,

$$R = \frac{I_{PPP,incoh} + I_{PPP,coh,sph}}{I_{SPP,incoh}} = 1 + \frac{I_{PPP,coh,sph}}{I_{SPP,incoh}}, \text{ for spherical symmetry,} \quad (2)$$

$$R = \frac{I_{PPP,incoh} + I_{PPP,coh,nonsph} + I_{PPP,coh,sph}}{I_{SPP,incoh} + I_{SPP,coh,nonsph}}, \text{ for any type of H - bond spatial arrangement,} \quad (3)$$

where *incoh* in the subscripts denotes an incoherent contribution, *coh, nonsph* and *coh, sph* denote coherent contributions from spherically correlated molecules and from non-spherically correlated molecules, respectively. The excess amount of PPP SH intensity over SPP SH intensity [Fig. 2(b)] can then be attributed to two possible factors. From Eq. (2) we derive that the intermolecular orientational correlations should increase with increasing temperature. This, however, is counter-intuitive because there are less H-bonds and intermolecular correlations with increasing temperature [Fig. 2(a)]. Then, using Eq. (3) an increase in the ratio R with increasing temperature can arise from a reduction in the amount of non-spherical orientational correlations combined with a relative increase in the amount of spherical orientational correlations. This makes sense because the H-bond network of water loses structure when temperature is increased.[43–46] The larger ratio R of D_2O thus indicates relatively more spherical intermolecular correlations than H_2O.

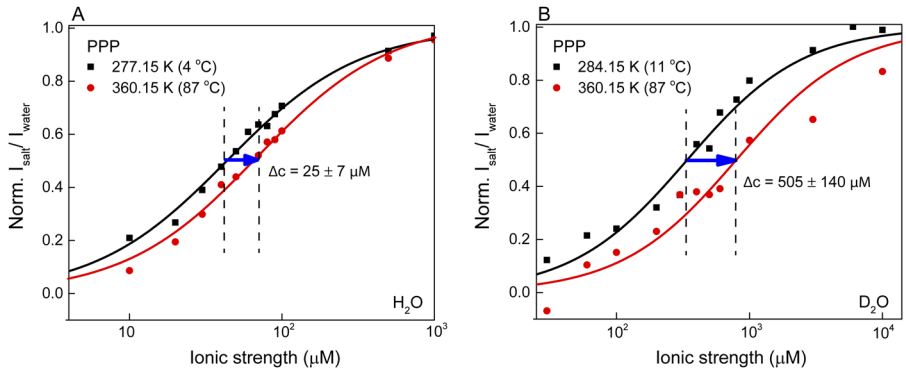

FIG. 3. fs-ESHS temperature dependence of NaCl solutions in light and heavy water. (a) Normalized SH Intensity (I_{salt}/I_{water}) of H_2O as a function of ionic strength at (277.15 K, 4 °C) and (321.15 K, 87 °C) measured at a scattering angle of 90° (PPP polarization combination). (b) Normalized SH Intensity (I_{salt}/I_{water}) of D_2O as a function of ionic strength at (284.15 K, 11 °C) and (321.15 K, 87 °C) measured at a scattering angle of 90° (PPP polarization combination). The solid lines are fits to the Debye-Hückel model.

The differences between D_2O and H_2O in Fig. 2, with the incoherent contributions removed, are manifestations of nuclear quantum effects. With H having a smaller mass than D, the nuclear quantum effect in H_2O is stronger than in D_2O. Nuclear quantum effects weaken the bending/libration mode of the H-bond and lead to less orientational order in H_2O compared to D_2O.[21,22,25,34,47] At 321.15 K (48.3 °C), the measured PPP SH intensity of D_2O is ~61% larger than that of H_2O. At 263.45 K (−9.8 °C), the measured PPP SH intensity of D_2O is ~53% larger than that of H_2O. Recent X-ray Raman scattering,[47] X-ray absorption spectroscopy,[37,48] and X-ray emission spectroscopy[49,50] studies of the molecular structures of liquid H_2O and D_2O show that there is enhanced asymmetry in the asymmetric H-bonds for H_2O compared to D_2O due to nuclear quantum effects. These findings agree with this study.

Temperature dependence of ion-water interactions

In a second set of experiments, we measured the temperature dependence of the water-water orientational correlations induced by ions in NaCl solution in H_2O and D_2O. Figure 3 shows the normalized fs-ESHS intensity as a function of ionic strength in H_2O [Fig. 3(a)] and D_2O [Fig. 3(b)], comparing the effects of Na^+ and Cl^- ions at the temperatures of maximum density for H_2O (277.15 K, 4 °C) and D_2O (284.15 K, 11 °C) to a fixed high temperature (321.15 K, 87 °C). As can be seen, there is a significant temperature effect in both solvents: Increasing the solution temperature shifts the increase in the SH intensity to higher ionic strength. The half-saturation points (c^*) in these curves change from $c^*(4\ °C) = 44 \pm 5\ \mu M \rightarrow c^*(87\ °C) = 69 \pm 5\ \mu M$ ($\Delta c^* = 25 \pm 7\ \mu M$) for H_2O and $c^*(4\ °C) = 300 \pm 51\ \mu M \rightarrow c^*(87\ °C) = 805 \pm 130\ \mu M$ ($\Delta c^* = 505 \pm 140\ \mu M$) for D_2O. Note that the c^* values at room temperature are at $55 \pm 5\ \mu M$ and $310 \pm 71\ \mu M$. The shift in the SH intensity curves indicate a weakened influence of the electrostatic fields of the ions on the water structure induced by increasing the temperature. The temperature dependent change in concentration can be qualitatively explained by the Debye-Hückel model.[18] With increasing temperature, the Debye length $(\kappa_D{}^{-1} = \left(\frac{\varepsilon_0 \varepsilon k T}{2N_A I 10^3 e^2}\right)^{1/2}$, where k is the Boltzmann constant, T the temperature in the unit K, N_A the Avogadro number, and I the ionic strength) increases, leading to a reduction of the influence of ions on the orientational correlations in the water. Additionally the ion induced dipole–dipole correlations have a temperature dependence of the form[27] $C(r) \sim \left(1/T^2\right) \exp\left(-\kappa_D r\right)/r$. Here, an increase of temperature results in a reduction of the dipole-dipole correlations. Together, these effects result in[18] $c^* = \frac{q^2 \varepsilon_0 \varepsilon k_B T}{2(Ze)^2}$, where q is the magnitude of the scattering vector and Z is the valence of the considered ion.

As such, a shifted intensity curve is expected. However, the model predicts $\Delta c^* = \sim 13\ \mu M$ and $\Delta c^* = \sim 80\ \mu M$ shifts in the ionic strength for H_2O and D_2O, respectively, using the measured values for c^* at the maximum density temperatures as input values. This qualitative agreement shows that the Debye-Hückel model can partially capture the temperature dependence of the ions' influence on the water structure. Although the direction of the shift in c^* is in the correct direction, for both H_2O and D_2O, the degree of change is significantly different. The screening capacity of the liquid is larger than that predicted for both liquids and relatively more for D_2O than for H_2O. This is surprising and somewhat counter-intuitive as one might expect that with higher temperatures H-bonds become weaker and so the influence of the electrostatic field on the orientational correlations would be reduced. That we observe the opposite suggests that there are more complicated interactions than the ones considered here. Indeed, the Debye-Hückel theory is not sophisticated enough to achieve a quantitative agreement. The underlying reason for that is that the model neglects any form of H-bonds. Also, nuclear quantum effects are not captured by the Debye-Hückel theory.[18] As recent computational studies show the importance of instantaneous fluctuations in the local H bond structure and since minute millidegree changes in the orientational order of water can already significantly impact the SH intensity,[18] these measurements provide a future opportunity for water models that should include both quantum effects and detailed non-local structures.[51]

CONCLUSIONS

In summary, using fs-ESHS we observed clear temperature dependent changes in the molecular structure of the

water H-bond network. The ensemble orientational order of water molecules decreases as the temperature increases. H_2O and D_2O show differences in their temperature dependence of the molecular structure of the H-bond network. With stronger H-bonding, D_2O has a more structured H-bond network in which molecular correlations exhibit relatively more spherical symmetry compared to H_2O. An increase in the temperature leads to a transformation of molecular correlations in pure water from correlations with non-spherical symmetry (e.g., single donor species) toward correlations with spherical symmetry (e.g., double donor species). For electrolyte solutions, we measured temperature dependent SH intensity versus concentration curves that show a decrease in the influence of the combined electrostatic field in the solution on the water-water correlations. The trend qualitatively follows the prediction from the Debye-Hückel theory, but the effects are larger than predicted: $\Delta c^* = 25\ \mu M$ for H_2O and $\Delta c^* = 505\ \mu M$ for D_2O were measured while the Debye-Hückel theory predicts $\Delta c^* = 13\ \mu M$ for H_2O and $\Delta c^* = 80\ \mu M$ for D_2O. Since the SH response can be computed from molecular dynamics simulations, the present observations provide a unique opportunity to refine quantum mechanical models of water.

ACKNOWLEDGMENTS

This work was supported by the Julia Jacobi Foundation and the European Research Council (Grant No. 616305). We thank D. M. Wilkins and M. Ceriotti for discussions.

[1] P. Ball, Chem. Rev. **108**, 74 (2008).
[2] Y. Marcus, *Ion Properties* (Marcel Dekker, New York, 1997).
[3] D. J. Tobias and J. C. Hemminger, Science **319**, 1197 (2008).
[4] W. Kunz, Pure Appl. Chem. **78**, 1611 (2006).
[5] Y. J. Zhang and P. S. Cremer, Annu. Rev. Phys. Chem. **61**, 63 (2010).
[6] P. Jungwirth and P. S. Cremer, Nat. Chem. **6**, 261 (2014).
[7] S. Funkner *et al.*, J. Am. Chem. Soc. **134**, 1030 (2012).
[8] G. Stirnemann *et al.*, J. Am. Chem. Soc. **135**, 11824 (2013).
[9] A. W. Omta *et al.*, Science **301**, 347 (2003).
[10] K. J. Tielrooij *et al.*, Science **328**, 1006 (2010).
[11] R. Buchner, G. T. Hefter, and P. M. May, J. Phys. Chem. A **103**, 1 (1999).
[12] J. D. Smith, R. J. Saykally, and P. L. Geissler, J. Am. Chem. Soc. **129**, 13847 (2007).
[13] I. Waluyo *et al.*, J. Chem. Phys. **140**, 244506 (2014).
[14] S. Bouazizi *et al.*, J. Phys. Chem. B **110**, 23515 (2006).
[15] I. Howell and G. W. Neilson, J. Phys.: Condens. Matter **8**, 4455 (1996).
[16] Y. Chen *et al.*, Phys. Chem. Chem. Phys. **19**, 24678 (2017).
[17] R. Mancinelli *et al.*, Phys. Chem. Chem. Phys. **9**, 2959 (2007).
[18] Y. Chen *et al.*, Sci. Adv. **2**, e1501891 (2016).
[19] J. A. Morrone and R. Car, Phys. Rev. Lett. **101**, 017801 (2008).
[20] B. Chen *et al.*, Phys. Rev. Lett. **91**, 215503 (2003).
[21] M. Ceriotti *et al.*, Chem. Rev. **116**, 7529 (2016).
[22] R. H. McKenzie *et al.*, J. Chem. Phys. **140**, 174508 (2014).
[23] F. Giberti *et al.*, J. Phys. Chem. B **118**, 13226 (2014).
[24] F. Paesani *et al.*, J. Phys. Chem. Lett. **1**, 2316 (2010).
[25] X. Z. Li, B. Walker, and A. Michaelides, Proc. Natl. Acad. Sci. U. S. A. **108**, 6369 (2011).
[26] F. Paesani and G. A. Voth, J. Phys. Chem. B **113**, 5702 (2009).
[27] D. M. Wilkins *et al.*, J. Chem. Phys. **146**, 181103 (2017).
[28] H. I. Okur *et al.*, Chem. Phys. Lett. **684**, 433 (2017).
[29] G. Gonella *et al.*, J. Phys. Chem. Lett. **3**, 2877 (2012).
[30] D. Marx, ChemPhysChem **8**, 209 (2007).
[31] S. Habershon, T. E. Markland, and D. E. Manolopoulos, J. Chem. Phys. **131**, 024501 (2009).
[32] T. E. Markland and B. J. Berne, Proc. Natl. Acad. Sci. U. S. A. **109**, 7988 (2012).
[33] D. Marx, A. Chandra, and M. E. Tuckerman, Chem. Rev. **110**, 2174 (2010).
[34] A. Soper and C. Benmore, Phys. Rev. Lett. **101**, 065502 (2008).
[35] Y. Nagata *et al.*, Phys. Rev. Lett. **109**, 226101 (2012).
[36] J. Liu *et al.*, J. Phys. Chem. C **117**, 2944 (2013).
[37] P. Wernet *et al.*, Science **304**, 995 (2004).
[38] N. Gomopoulos *et al.*, Opt. Express **21**, 815 (2013).
[39] G. A. Vidulich, D. F. Evans, and R. L. Kay, J. Phys. Chem. **71**, 656 (1967).
[40] C. Liang *et al.*, Phys. Rev. B **96**, 041407(R) (2017).
[41] R. Bersohn, Y. H. Pao, and H. L. Frisch, J. Chem. Phys. **45**, 3184 (1966).
[42] Y. Chen and S. Roke, e-print arXiv:1705.04231 (2017).
[43] K. Modig, B. G. Pfrommer, and B. Halle, Phys. Rev. Lett. **90**, 075502 (2003).
[44] T. Head-Gordon and G. Hura, Chem. Rev. **102**, 2651 (2002).
[45] J. G. Davis *et al.*, Nature **491**, 582 (2012).
[46] Y. Marcus, Chem. Rev. **109**, 1346 (2009).
[47] U. Bergmann *et al.*, Phys. Rev. B **76**, 024202 (2007).
[48] A. Nilsson and L. G. M. Pettersson, Chem. Phys. **389**, 1 (2011).
[49] C. Huang *et al.*, Proc. Natl. Acad. Sci. U. S. A. **106**, 15214 (2009).
[50] T. Tokushima *et al.*, J. Electron Spectrosc. Relat. Phenom. **177**, 192 (2010).
[51] P. Hünenberger and M. Reif, *Single-Ion Solvation: Experimental and Theoretical Approaches to Elusive Thermodynamic Quantities* (Royal Society of Chemistry, 2011).